Experimental Neurology 311 (2019) 182–193

Contents lists available at ScienceDirect

Experimental Neurology

journal homepage: www.elsevier.com/locate/yexnr

Research Paper

A Mesenchymal stem cell line (B10) increases angiogenesis in a rat MCAO model

Abdullah Md. Sheikh[a], Shozo Yano[a], Shingo Mitaki[b], Md. Ahsanul Haque[b], Shuhei Yamaguchi[b], Atsushi Nagai[a,*]

[a] Department of Laboratory Medicine, Shimane University School of Medicine, 89-1 Enya Cho, Izumo 693-8501, Japan
[b] Department of Neurology, Shimane University School of Medicine, 89-1 Enya Cho, Izumo 693-8501, Japan

ARTICLE INFO

Keywords:
Mesenchymal stem cell line (B10)
Transplantation
Angiogenesis
MCAO
HIF-1α
VEGF
IL-1β

ABSTRACT

A human mesenchymal stem cell line (B10) transplantation has been shown to improve ischemia-induced neurological deficits in animal stroke models. To understand the underlying mechanism, we have investigated the effects of B10 transplantation on cerebral angiogenesis in a rat middle cerebral artery occlusion (MCAO) model. B10 cells were transplanted intravenously 24 h after MCAO. Immunofluorescence staining results showed that compared to PBS-groups, vWF positive vessel and endoglin positive new vessels were increased in B10-transplanted MCAO groups in the lesion areas. The mRNA of angiogenesis factors including placental growth factor and hypoxia inducible factor (HIF)-1α were increased 3 days after MCAO in the core and IBZ areas of B10-transplanted group. Angiopoetin1 mRNA was increased only in the IBZ. Western blotting results showed that HIF-1α and vascular endothelial growth factor (VEGF) proteins were increased in B10-transplanted group. Both HIF-1α and VEGF were expressed in macrophage/microglia in the core area. In the IBZ, however, HIF-1α was expressed both in astrocytes and macrophage/microglia, while VEGF was expressed only in macrophage/microglia. Moreover, TGFβ protein levels were found to be increased in B10-transplanted group in the core and IBZ regions. Cell culture experiments using a human microglia cell line (HMO6) and B10 showed that IL-1β induced VEGF mRNA expression in both cell types. IL-1β was found to be highly expressed in B10 cells, and its co-culture with HMO6 further increased that in B10. Co-culture increased VEGF mRNA in both B10 and HMO6. In the rat brains, IL-1β was expressed in macrophage/microglia and transplanted-B10 cells in the core. IL-1β positive cell number was increased slightly, but significantly in B10-transplanted rats. To explore further, IL-1β expression was silenced in B10 cells by transfecting mRNA specific siRNA, and then transplanted in MCAO rats. Immunostaining result showed that endoglin positive area was decreased in IL-1β-silenced B10 transplanted groups compared to nonsilenced-B10 transplanted groups. Interestingly, vessel-like structure appeared as early as 3 days after MCAO in IL-1β-silenced B10-transplanted group. Thus our results demonstrated that B10 cells increased angiogenesis in MCAO rat model, through the regulation of HIF-1α and VEGF expression, where IL-1β might play a role.

1. Introduction

Brain tissue is highly dependent on oxygen for its energy metabolism, and consequently can tolerate oxygen deprivation only for a short period of time (Bélanger et al. 2011; Kumar et al. 2010). Cerebral vasculature is developed uniquely by making an elaborate arteriolar anastomotic network. Such vascular arrangement helps to protect brain tissue during conditions of decreased blood supply through anastomotic collateral circulation (Liebeskind 2003). Stroke occurs due to severe interruption of cerebral blood flow that generally results from blockage of an artery(s) and critical reduction of perfusion to the supply area that cannot be compensated by the collateral circulations (Bang et al. 2015). After blockage of the artery, the perfusion-compromised area undergoes necrosis (Kumar et al. 2010). Then, a highly interactive process of inflammation and repair system is activated, as evidenced by infiltration of inflammatory cells, along with induction of angiogenesis, neurogenesis and synaptogenesis (Ceulemans et al. 2010). Several reports have demonstrated that post-stroke neurogenesis depends significantly on neovascularization, implying a coordinated work of these processes that orchestrate a neurological recovery (Ohab et al. 2006; Thored et al.

* Corresponding author.
E-mail address: anagai@med.shimane-u.ac.jp (A. Nagai).

https://doi.org/10.1016/j.expneurol.2018.10.001
Received 18 December 2017; Received in revised form 29 August 2018; Accepted 1 October 2018
Available online 03 October 2018

2007; Xiong et al. 2011). Furthermore, histological data of stroke patients showed the importance of angiogenesis and vascular remodeling in the ischemic area, where higher blood vessel density in the stroke area indicates a better prognosis (Krupinski et al. 1994). Also, the therapy that increases angiogenesis has been shown to be beneficial in animal models of stroke (Sun et al. 2003). Hence, angiogenesis in the stroke condition might be a good target for the therapy of the disease.

Angiogenesis is an important process for forming new blood vessels, manifested by extensive interactions between a wide variety of molecules including growth factors, cytokines, adhesion molecules, chemokines, enzymes and activators and inhibitors of angiogenesis (Carmeliet and Jain 2011). In response to specific activators such as hypoxia or inflammation, angiogenesis regulators are expressed in the affected regions, causing the sprouting of vessels from existing one, and ultimately new vessels are formed (Carmeliet and Jain 2011). Several angiogenesis regulators including VEGF, βFGF, angiopoietins and Tie2 are found to be expressed in stroke condition, suggesting that an angiogenic process is activated in the affected areas (Wang et al. 2002; Zhang and Chopp 2015). This hypothesis is supported by the fact that new vessels are formed in the stroke area along with time dependent expression of angiogenesis regulators (Buga et al. 2014; Krupinski et al. 1994). Such process appears to be important for neurogenesis and neuroprotection as it was shown that new neurons are frequently found near the area of angiogenesis (Ohab et al. 2006; Thored et al. 2007).

Recently stem cell transplantation-based therapies are gaining much interest because of their ability to replace damaged neurons, neuroprotection, immunomodulation and angiogenesis (Chen et al. 2003; Chen et al. 2004; Sheikh et al. 2011). Among the stem cell types used for stroke therapy, mesenchymal stem cells might be important because of its ability to produce growth factors, induce neuronal differentiation and modulate neuroinflammation (Nagai et al. 2007; Sheikh et al. 2011; Wakabayashi et al. 2010). In our previous study, we have found that a mesenchymal stem cell line transplantation increased VEGF mRNA expression along with many other growth factors in vivo in a MCAO rat model (Wakabayashi et al. 2010). Moreover, the analysis of MSC secretome shows that it can produce several angiogenic factors (Bakopoulou et al. 2015). Therefore, we hypothesized that MSC could modulate the angiogenesis system in stroke condition. To test this hypothesis, we transplanted a mesenchymal stem cell line in a rat stroke model and examined angiogenesis, and the regulation of its underlying mechanism. We found that the transplantation increased vessel density in the stroke area possibly through increased expression of HIF-1α and other angiogenesis factors.

2. Materials and methods

2.1. Cell culture

Bone marrow cells were isolated from human fetal spinal vertebrae, and immortalized by introducing v-*Myc* oncogene using a retroviral vector (Nagai et al. 2007). A clone (B10) of immortalized bone marrow cells, which showed similar morphological and expressional phenotype and differentiation potentials as primary human mesenchymal stem cells, was expanded. This human mesenchymal stem cell line was cultured in complete MF® medium (Toyobo, Osaka, Japan) containing 1% FCS and growth factor supplement (Wakabayashi et al. 2010).

Human primary microglia were isolated from human fetal brain and immortalized by transfecting a retroviral vector encoding v-*Myc*, as described previously (Nagai et al. 2001). A clone (HMO6), which shows similar morphological and expressional phenotype like primary microglia, was expanded. HMO6 was cultured in Dulbecco's modified Eagle medium (DMEM, Gibco, Invitrogen, Carlsbad, CA) of high glucose concentration, supplemented with 5% fetal bovine serum (Gibco), L-glutamine and antibiotics (Gibco) (Nagai et al. 2001). During cytokine treatment, 0.5% FBS containing DMEM was used for both B10 and HMO6 cells. For oxygen glucose deprivation (OGD) experiments, cells were incubated in an incubator in humid condition at 37 °C, with 0.1% O_2 and 5% CO_2 for 4 h. The composition of OGD medium was: NaCl 116 mM, KCl 5.4 mM, $MgSO_4$ 0.8 mM, KH_2PO_4 0.44 mM, $CaCl_2$ 1.2 mM, $NaHCO_3$ 20 mM, Na_2HPO_4 0.33 mM, and Phenol Red 10 mg/l.

To investigate about the effect of B10 on microglia, a co-culture system of HMO6 and B10 was developed. HMO6 cells were cultured in a well of 6-well cell culture plate and B10 cells were in a cell culture insert (Millipore, Billerica, MA). After confluency, B10 cell containing cell culture insert was placed in the well of HMO6, resulting free movement of cell culture secreting molecules through the pores. However, there was no physical contact between B10 and HMO6 cells. DMEM medium containing 0.5% FBS was added and co-culture was continued up to 36 h.

2.1.1. Silencing IL-1β in B10 cells

To silence human IL-1β mRNA expression, gene-specific silencing siRNA (Qingen, Valencia, CA) was transfected into B10 cells using HiPerfect transfection reagent (Qiagen) according to the manufacturer's protocol after optimizing the condition. For transfection, 10 nM siRNA and 3 μl HiPerfect transfection reagent was used for 1 well of 24-well plate. When transfection was done in 100 mm dishes, the amount of Hiperfect reagent was increased proportionate to the surface area. Forty-eight hours after transfection, cell culture medium was changed with 0.5% FBS containing DMEM and cultured for further 24 h. Then the silencing effect was determined by real-time PCR and ELISA.

2.2. Animal model of focal ischemia

Animal care was done according to the guidelines of the experimental institute of Shimane University. All animals were kept under a constant temperature (23 ± 2 °C) and a light-dark cycle of 12 h. The animals were fed with commercially available normal rat diet and tap water ad libitum. All experimental protocol and procedures were approved by the Ethical Committee of Shimane University School of Medicine, and were done following the guideline of the experimental animal institute of Shimane University. Adult male Wister rats (Charles River, Yokohama, Japan), weighing 250 to 300 g, were used in this study. Transient focal cerebral ischemia was induced following an established method described previously (Wakabayashi et al. 2010). Briefly, rats were anesthetized with 4% halothane. Then the common, external and internal carotid arteries were exposed through a ventral midline incision. A silicon coated 4–0 monofilament nylon suture with rounded tip was inserted through the right common carotid artery, and advanced until it occluded the middle cerebral artery. Then the anesthesia was reversed, and the rats were kept in a cage. After 90 min of occlusion, the rat was re-anesthetized and the nylon suture was withdrawn. Rectal temperature was maintained around 37 °C throughout the surgical procedure using a feedback-regulated heating system.

2.3. Intravenous injection of B10 human mesenchymal stem cells

One day after MCAO, the rats were neurologically evaluated using a previously described neurological severity scoring system (Wakabayashi et al. 2010). Rats of similar neurological severity score were randomly divided into 3 groups (n = 5 for each time point and experiment type) to receive B10 cells, IL-1β-silenced B10 cells or phosphate buffered saline (PBS). IL-1β-silenced B10 cells were transplanted 24 h after transfection of siRNA. For transplantation, a rat was anesthetized with 4% halothane, the jugular vein was exposed, and 3×10^6 cells in 100 μl of PBS or PBS-alone was injected (Wakabayashi et al. 2010). The tissue of a total 60 MCAO rats (25 for PBS-treated groups, 25 for B10 transplanted groups and 10 for IL-1β-silenced B10 transplanted groups) was used in this study.

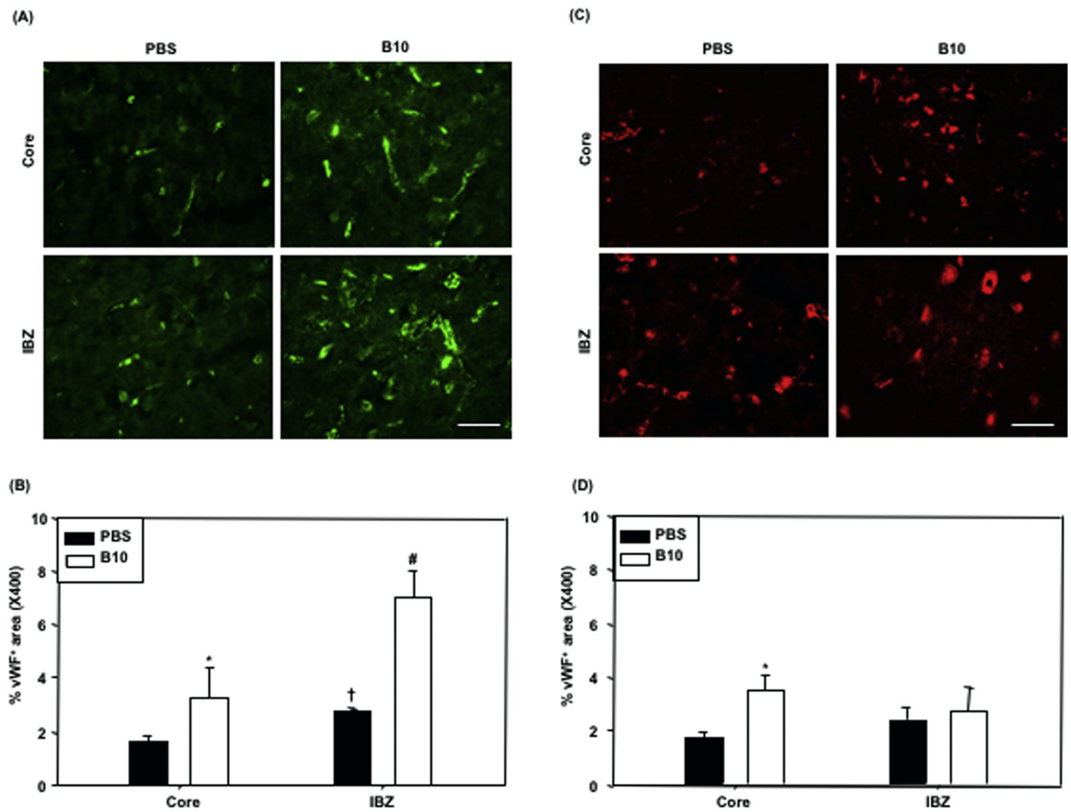

Fig. 1. Effects of B10 transplantation on angiogenesis in a MCAO rat model. B10 cells were transplanted intravenously 24 h after MCAO. Control MCAO rats received PBS instead of cells. Three and 7 days after MCAO, vessels in the core and IBZ region were visualized by vWF immunofluorescence staining. Vessel density was evaluated using ImageJ, as described in the Materials and Methods, and expressed as percent of total area of a microscopic field at x400 magnification. Representative vWF immunofluorescence staining photomicrographs of ischemic core and IBZ cortices of rat brains 3 and 7 days after MCAO are shown in (A) and (C), respectively. Quantified data of the staining of rat brains 3 (B) and 7 (D) days after MCAO are presented as average of 5 rats ± SD. Statistical significance are denoted as follows; $^{*}p < 0.05$ vs same area of PBS (control) rats, $^{\#}p < 0.001$ vs same area of PBS (control) rats, $^{\dagger}p < 0.001$ vs core area of PBS (control) rats.

2.4. Immunohistochemical analysis

Three, seven and 14 days after MCAO, rats were deeply anesthetized with isoflurane, and perfused transcardially with normal saline followed by 4% paraformaldehyde in 0.1 M phosphate buffer to fix the tissue. Then the brains were removed, postfixed with same fixative, cryoprotected with 30% sucrose, and tissue blocks of 2 mm thickness were sectioned. For staining, a tissue slice of 10 μm thickness was sectioned on a cryostat. After quenching endogenous peroxidase activity, the sections were incubated in a blocking solution containing 10% normal goat or horse serum and 0.2% Triton X-100 in PBS. Then the sections were incubated with anti-von-willebrand factor (vWF) IgG (rabbit, 1:100, Dako, Carpinteria, CA), anti-endoglin (CD105) IgG (goat, 1:200, R&D, Minneapolis, MN) anti-Iba-1 IgG (rabbit, 1:200, Wako, Richmond, VA), anti-HIF-1α IgG (Mouse, 1:200 Santa Cruz, Santa Cruz, CA), anti GFAP IgG (rabbit, 1:200, Dako), anti-p300 IgG (rabbit, 1:200, Santa Cruz), anti-VEGF IgG (goat, 1:100, Santa Cruz), anti-TGFβ IgG (rabbit, 1:100, Dako), anti-IL-1β (goat, 1:200, Santa Cruz) and anti-human nuclei IgG (mouse, 1:100, Millipore). In the case of immunofluorescence staining, the tissue sections were then incubated with Texas red-conjugated or FITC-conjugated species-specific IgG, and nuclei were stained with Hoechst. For light microscopy, the section was incubated with biotin-conjugated species-specific IgG (1:100, Vector, Ingold Road, CA), followed by incubation with an avidin–biotin–peroxidase complex (ABC, Vector). The immune reaction products were visualized with 3, 30-diaminobenzidine (DAB, Sigma, St. Louis, MO), and the tissue was counterstained with Haematoxylin. Stained sections were examined under a fluorescent microscope (NIKON, ECLIPSE E600). For counting the cells, 3 tissue sections of 2 mm apart were stained, and cells were randomly counted in 5 microscopic field of designated area at X400 magnification in a blinded manner. The average cell number of a total 15 fields represented the cell number in that area of the rat brain. To determine vessel density in 3 and 7 days MCAO models, 3 tissue sections of 2 mm apart were immunostained with vWF, photomicrographs of 5 random microscopic fields at X400 magnification in the core and IBZ regions were taken, and analyzed the immunostained area by ImageJ software. The vessel density was calculated as percent of immunostained area occupied in a microscopic field. The average percent area of a total 15 fields represented the vessel density in that area of the rat brain.

2.5. Total RNA isolation, reverse transcription and quantitative real time PCR

Total RNA was isolated from cultured cells after appropriate treatment, or from infarct core, cortical ischemic border zone (IBZ) or contralateral cortex of PBS-treated or B10-transplanted rat brains 3 days after MCAO, using Trizol reagent (Invitrogen) according to the manufacturer's instructions. To prepare first strand cDNA, 2 μg of total RNA was reverse transcribed with reverse transcriptase enzyme (RiverTraAce, Toyobo, Osaka, Japan) in a 20 μl reaction mixture. To analyze mRNA level, real time PCR was performed with SyBr green PCR system (Power SyBr green, Applied Biosystem, Warrington, UK) using an ABI Prism 7300 Sequence Detector system (Applied Biosystems). To detect mRNA of rat origin, real time PCR primers were designed using sequences of rat mRNA regions that are not in homology with human mRNA sequences of same gene (Wakabayashi et al. 2010). The mRNA level was normalized by corresponding GAPDH mRNA and quantified

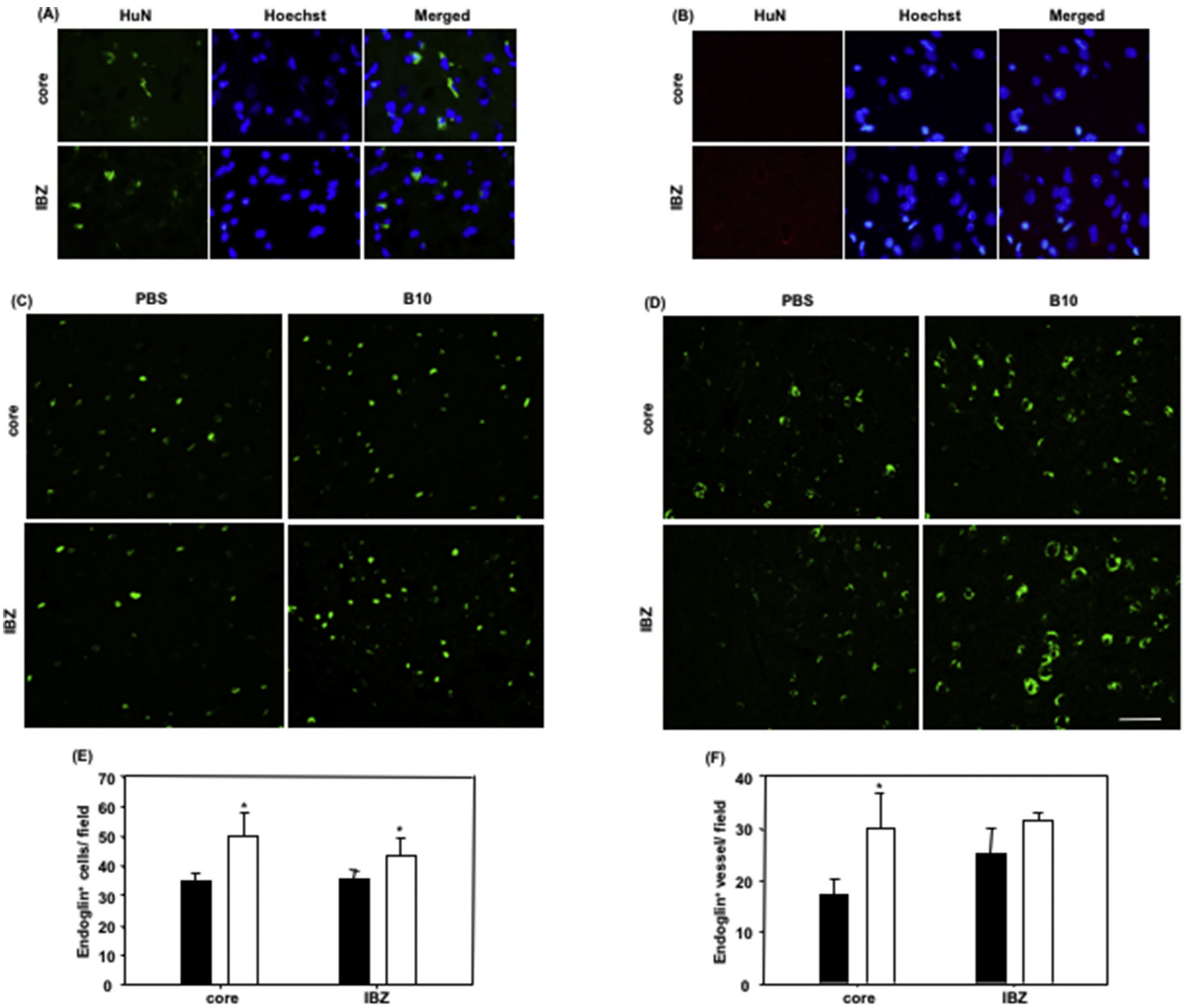

Fig. 2. Detection of transplanted B10 cells and newly formed vessels in the brains of MCAO rats. B10 cells were transplanted intravenously 24 h after MCAO. Control MCAO rats received PBS instead of cells. Three and 7 days after MCAO, B10 in the core and IBZ region were visualized by human nuclear antigen (HuN) immunofluorescence staining. Similarly, newly formed vessels were identified by endoglin immunofluorescence staining. Endoglin immunofluorescence was evaluated using ImageJ, as described in the Materials and Methods. Representative HuN immunofluorescence photomicrographs of ischemic core and IBZ cortices of rat brains, 3 days (C) and 7 days (D) after MCAO are shown, and quantified data of the staining of 3 days (B) and 7 days (D) after MCAO are presented in (E) and (F), respectively. The quantified data are presented here as average ± SD of 5 rats in a group. Statistical significance are denoted as follows; $*p < 0.05$ vs same area of PBS (control) rats. Bar = 50 μm.

using relative quantification method.

2.6. Western blot analysis

Total protein was isolated from cultured cells after appropriate treatment, or from infarct core, IBZ or contralateral cortex of PBS-treated or B10-transplanted rat brain 3 days after MCAO using ice cold RIPA buffer (PBS, pH 7.4, 1% Nonidet p-40, 0.5% sodium deoxycholate, 0.1%SDS, 10 mg/ml PMSF, and 1 mg/ml aprotinin). To homogenize brain tissue, 20× wt/vol of RIPA buffer was used. Twenty to 60 μg of total protein was separated by SDS polyacrylamide gel electrophoresis, transferred to a PVDF membrane (Millipore, Billerica, MA). After blocking, the membrane was incubated with anti-HIF-1α (mouse, Santa Cruz), anti-p300 (rabbit, Santa Cruz), anti-VEGF (goat, Santa Cruz) or anti-TGFβ (rabbit, Dako) IgG. Then the membrane was incubated with infrared (IR) fluorophore-conjugated species-specific IgG (Li-Cor, Lincoln, NE). Immunoreactive proteins in the membrane were detected using an IR scanner (Li-Cor) according to the manufacturer's protocol.

2.7. ELISA

Culture supernatants were collected from the cell cultures, and the concentration of IL-1β was measured by sandwich ELISA using a human IL-1β platinum ELISA Kit (Invitrogen) according to the manufacturer's instructions. Briefly, culture supernatants were centrifuged at 14,000 rpm for 10 min at 4 °C to remove cell debris. Equal volume of sample diluent, provided by the manufacturer, was added to the culture supernatant. Then 100 μl of diluted samples were added to the wells of a 96-well plate coated with anti-IL-1β antibody and incubated at room temperature for 2 h. After wash, a biotin conjugated anti-human IL-1β antibody (100 μl) was added to the wells and incubated for 2 h at room temperature. Then HRP-conjugated streptavidin (100 μl) was added to the wells and incubated for 1 h at room temperature. After wash, TMB substrate (100 μl) was added to the wells and incubates at room temperature in a dark condition for 10 min. The reaction was terminated by adding a stop solution provided by the manufacturer, and optical densities were measured with a plate reader (EAR400, SLT-Lab instruments). IL-1β concentration was calculated after preparing a standard curve using human IL-1β standard (Invitrogen).

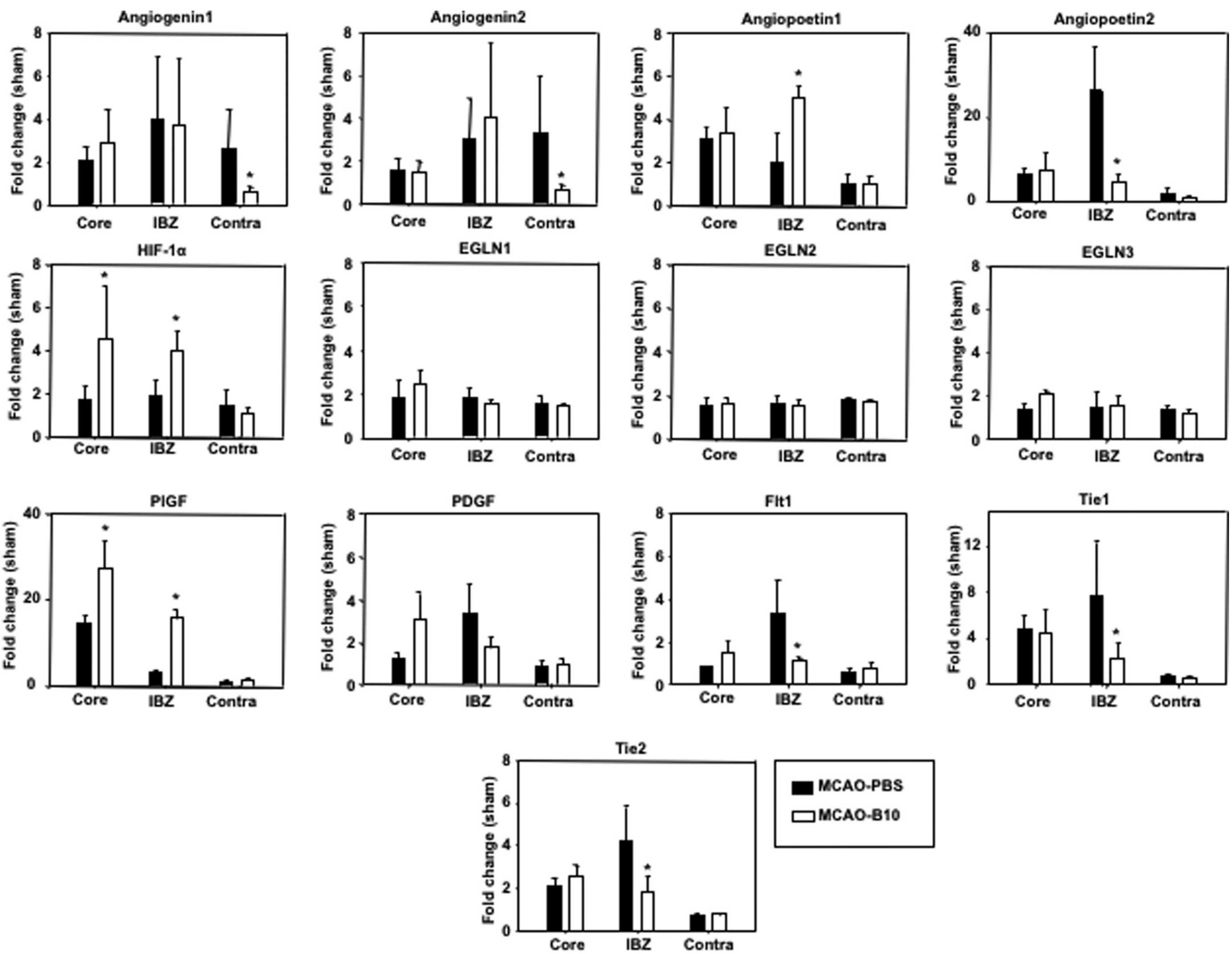

Fig. 3. Effects of B10 transplantation on the mRNA level of angiogenesis related factors in a MCAO rat model. B10 cells were transplanted intravenously 24 h after MCAO. Control MCAO rats received PBS instead of cells. Sham animals were undergone all surgical procedure except occlusion of the artery and transplantation. Three days after MCAO, cortical brain tissues from ischemic core, IBZ and contralateral areas were dissected out, total RNA was isolated, reverse transcribed, and mRNA levels of angiogenesis related factors were evaluated by real time PCR. The mRNA levels of target genes were normalized with those of corresponding GAPDH, calculated as fold induction relative to mRNA from cortex of a sham animal, and results are presented as mean ± SD of 5 rats. Statistical significance is denoted as follows; $*p < 0.05$, vs PBS (control) rats.

2.8. Statistical analysis

The numerical data are presented as mean ± SD. Statistical differences among the groups were assessed by one-way ANOVA followed by Scheffe's post hoc test, or paired *t*-test. The statistical significance level was set at $p < 0.05$.

3. Result

3.1. B10 transplantation increased angiogenesis in a rat MCAO model

In a previous report, we have shown that B10 transplantation increased VEGF mRNA expression in a rat MCAO model after 3 days (Wakabayashi et al. 2010). Hence, we chose to investigate angiogenesis starting at that time point. Staining of blood vessels with vWF antibody revealed that in PBS-treated MCAO rats, the vessel density was significantly decreased in the core region compared to ischemic border zone (IBZ) at 3 days (Fig. 1A and B). Compared to corresponding areas of PBS-treated group, B10-transplanted group showed increased vessel density in both ischemic core and IBZ region in the cortical areas at 3 days (Fig. 1A and B). At 7 days after MCAO, the difference sill persisted in the core region; however, the vessel density was similar in the IBZ area of PBS-treated and B10-transplanted groups (Fig. 1C and D). Also at 14 days, the difference of vessel density was found mainly in the core region (Supplemental Fig. 1).

3.2. Transplanted B10 cells localized in the ischemic area and increased newly formed vessels in rat MCAO model

Next, we analyzed the distribution of transplanted B10 cells in MCAO rat brains. Since it is a human origin mesenchymal stem cell line, we used antibody against human nuclear antigen (HuN) to identify transplanted B10 cells in rat host brains. In our previous studies, we have found that B10 cells mainly accumulated in the core and IBZ regions of the brains at 3 days after MCAO (Wakabayashi et al. 2010; Wang et al. 2013). The number was decreased at 5 days, and at 7 days after MCAO, no B10 cells were detectable (Wakabayashi et al. 2010; Wang et al. 2013). In this study also B10 cells were detectable in the core and IBZ region at 3 days (Fig. 2A), and no transplanted B10 cells were detectable at 7 days after MCAO in the rat brains (Fig. 2B).

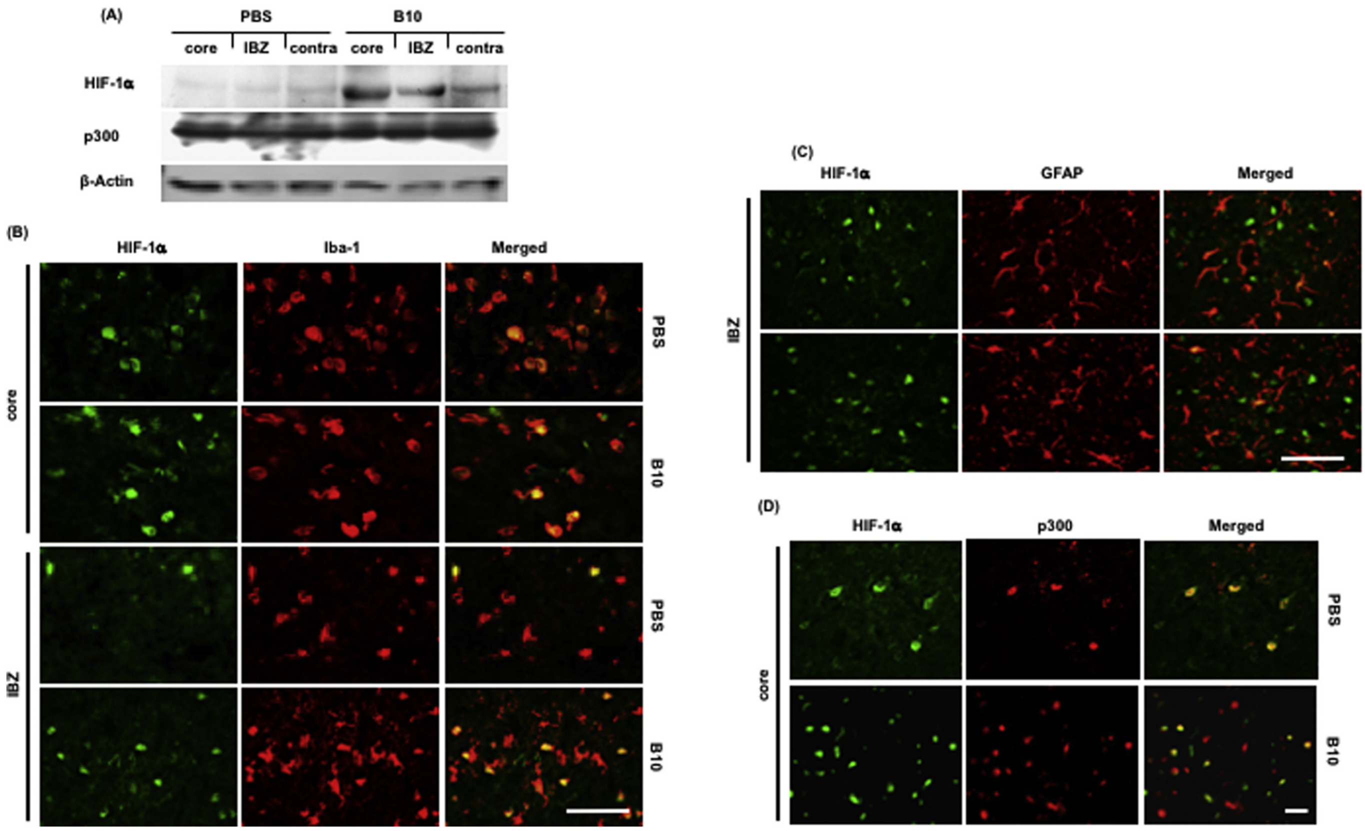

Fig. 4. Effects of B10 transplantation on HIF-1α protein expression in MCAO rat brains. B10 cells were transplanted intravenously 24 h after MCAO. Control MCAO rats received PBS instead of cells. Three days after MCAO, cortical brain tissues from ischemic core, IBZ and contralateral areas were dissected out, and levels of HIF-1α and p300 were evaluated by Western blot analysis using specific antibodies (A). β-Actin was used as a loading control (A). To determine the localization of HIF-1α, double immunofluorescence staining was done where Iba-1 (B) and GFAP (C) were used as astrocyte and macrophage/microglia markers, respectively. Co-localization of HIF-1α and p300 was determined by double immunofluorescence staining using specific antibodies (D). Bar = 50 μm in (B and C) and 20 μm in (D).

To analyze further about the effects of B10 transplantation on angiogenesis in MCAO condition, we evaluated newly formed vessels by endoglin immunostaining. Endoglin is suggested to be a better marker for newly formed vessels, whereas vWF can detect both newly formed and normal vessels (Yao et al., 2005). Immunostaining results showed that at 3 days after MCAO, endoglin positive cell number was increased in both core and IBZ areas of B10 transplanted rats (Fig. 2C and E). At 7 days after MCAO, endoglin stains adopted microvessel-like structures in the core and IBZ regions of both PBS and B10 transplanted rats (Fig. 2D). Moreover, some endoglin positive cells were present along with microvessel-like structure in B10 transplanted rats, especially in the core area. The average diameter of those miscrovessel-like structures were 23.6 μm (range 15–31.2 μm) and 25.9 μm (range 14.4–40.5 μm) in the core region of PBS-treated and B10 transplanted MCAO rats, respectively. In the IBZ region of PBS-treated and B10 transplanted rats, the average diameter was 31 μm (range 20–41.7 μm) and 28.3 μm (range 18.7–40.8 μm), respectively. Counting of these microvessel-like structures revealed that the number was significantly increased in the core region of B10 transplanted rats (Fig. 2F). At 14 days after MCAO, endoglin positive area was still increased in the core region of B10-transplanted rats. In the IBZ region of both PBS-treated and B10-transplanted rats, well-formed microvessels were seen at this time point (Supplemental Fig. 2).

3.3. *B10 transplantation affected the mRNA expression of angiogenesis-related genes in rat MCAO model*

Next, we have checked the mRNA expression of several angiogenesis-related factors in MCAO rat brains. The results revealed that the mRNA levels of angiopoetin2 (Ang2), placenta growth factor (PlGF) and Tie1 were considerably increased in PBS-treated MCAO rats brains, whereas the mRNA of angiopoetin1 (Ang1), HIF-1α and EGL-Nine homologs (EGLNs) were not increased much (Fig. 3). Compared to PBS-treated group, the mRNA levels of Ang1, HIF-1α and PlGF were significantly increased in the IBZ region of B10-transplanted group. In the core region of B10-transplanted group, the mRNA of HIF-1α and PlGF were increased. Conversely, compared to PBS-treated group, the expression of Ang2, Flt1, Tie1 and Tie2 mRNA was decreased in IBZ region of B10-transplanted group. However, the mRNA levels of EGLNs, the enzymes that regulate hypoxia-dependent stability of HIF-1α, were similar between 2 groups in all areas that we have checked.

3.4. *B10 transplantation increased HIF-1α protein level in a rat MCAO model*

Next, we investigated about the protein expression of HIF-1α. Western blotting results demonstrated that HIF-1α protein was barely detectable in the core, IBZ or contralateral cortical areas of PBS-treated MCAO rat brains 3 days after MCAO (Fig. 4A). However, a significant increase of HIF-1α protein was seen mainly in the core and IBZ region of B10-transplanted group (Fig. 4A). On the other hand, the level of p300, a coactivator of HIF-1α, was not changed (Fig. 4A). To analyze their localizations in B10-transplanted rat brain tissue, double immunofluorescence staining of HIF-1α and GFAP (astrocyte marker), or HIF-1α and Iba-1 (macrophage/microglia marker) were done. We did not find GFAP positive astrocytes in the core region of rat brains 3 days after MCAO, where Iba-1 positive macrophage/microglia were detected. In the IBZ region, both GFAP positive astrocytes and Iba-1 positive macrophage/microglia were detectable. In the core region, HIF-1α was expressed mainly in Iba-1 positive macrophage/microglia

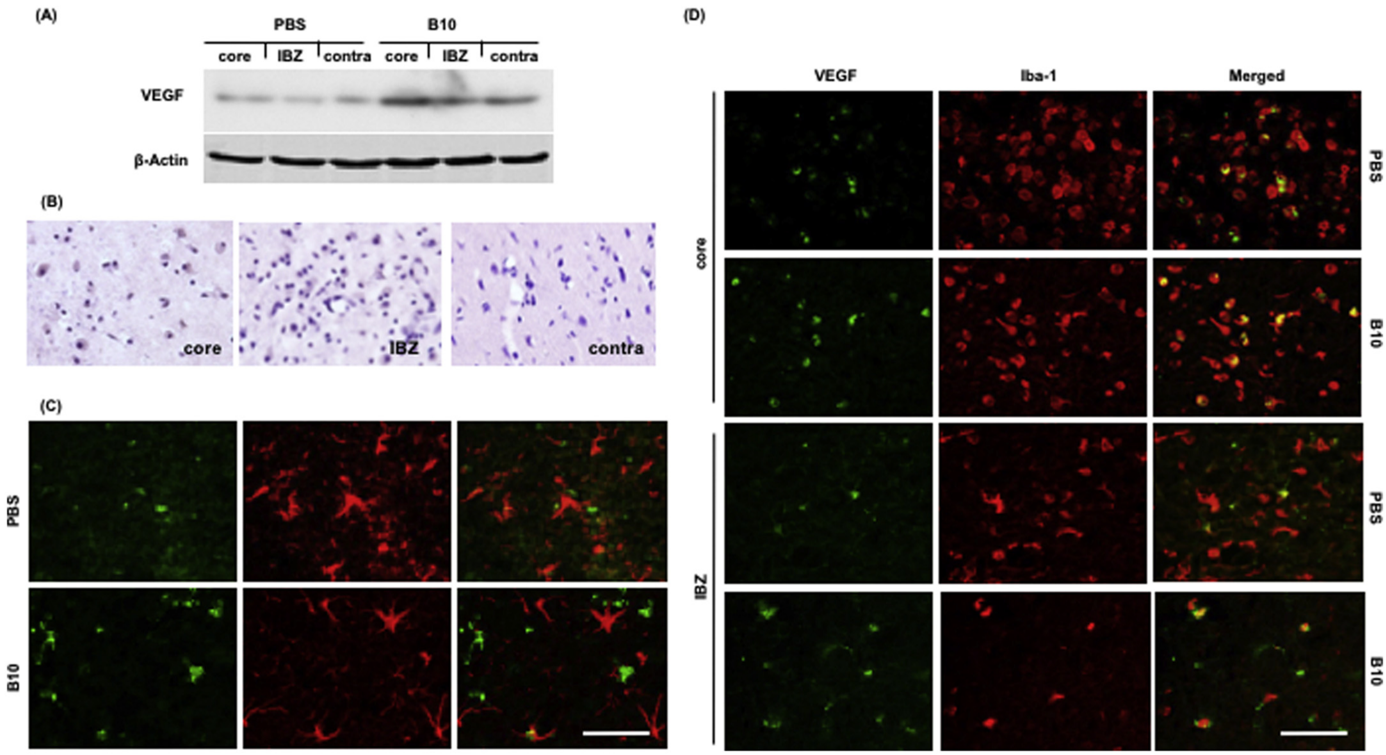

Fig. 5. Effects of B10 transplantation on VEGF protein expression in MCAO rat brains. B10 cells were transplanted intravenously 24 h after MCAO. Control MCAO rats received PBS instead of cells. Three days after MCAO, cortical brain tissues from ischemic core, IBZ and contralateral areas were dissected out, and level of VEGF was evaluated by Western blot analysis using specific antibody (A). β-Actin was used as a loading control (A). To determine the distribution and morphology of VEGF expressing cells in MCAO, immunostaining with specific antibody was done. Representative photomicrographs of cortical core, IBZ contralateral areas are shown in (B). Double immunofluorescence staining was done to identify VEGF-expressing cells where GFAP was used as astrocyte marker (C), and Iba-1 as macrophage/microglia marker (D). Bar = 50 μm.

(Fig. 4B). In the IBZ region, HIF-1α was found to be expressed in both GFAP positive astrocytes and Iba-1 positive macrophage/microglia (Fig. 4B and C). As p300 plays a role in HIF-1α activation (Ruas et al. 2010), we checked its co-localization with HIF-1α. The immunofluorescence results showed that indeed, p300 was co-localized with HIF-1α (Fig. 4D).

3.5. B10 transplantation increased VEGF protein level in a rat MCAO model

VEGF is a potent angiogenesis factor. As VEGF is a downstream target of HIF-1α (Forsythe et al. 1996), we checked its regulation by B10 transplantation in MCAO rat model. Western blotting results demonstrated that VEGF protein was detectable in the core, IBZ and contralateral cortices of PBS-treated rat brains 3 days after MCAO, which was increased in those areas in B10-transplanted rats (Fig. 5A). Immunostaining results showed that in the core and IBZ regions, VEGF expressed mainly in round shaped cells (Fig. 5B). Double immunofluorescence staining showed that VEGF expressed mainly in Iba-1 positive macrophage/microglia in both core and IBZ region of PBS-treated and B10-transplanted rats (Fig. 5C and D).

3.6. B10 transplantation increased TGFβ production in a rat MCAO model

Previous reports have shown that TGFβ plays an important role in the development of blood vessels (Nguyen et al. 2011). Hence, we checked the regulation of TGF production in MCAO rat model. Western blotting results showed that TGFβ protein level was undetectable in the contralateral cortex of the rats, whereas the protein was barely detectable in the core and IBZ cortical areas of PBS-treated rats 3 days after MCAO (Fig. 6A). The level of TGFβ was increased in the core and IBZ region in B10-transplanted rats (Fig. 6A). Immunofluorescence staining also confirmed the result, showing an increase of TGFβ expression in the core and IBZ region of B10-transplanted rats (Fig. 6B).

3.7. Regulation of VEGF expression in macrophage/microglia by B10

We investigated about the regulation of VEGF expression in macrophage/microglia by B10 cells using an in vitro cell culture system. In previous reports, it has been shown that inflammatory cytokines affect angiogenesis through production of VEGF (Asano-Kato et al. 2005). Our real-time PCR result showed that stimulation of a macrophage/microglia cell line (HMO6) or B10 with IL-1β time-dependently increased VEGF mRNA level (Fig. 7A and B). However, the peak of VEGF mRNA expression was 8 h in B10 and 24 h in HMO6 (Fig. 7A and B). Next, we checked the effects of B10 on HMO6 in respect of IL-1β and VEGF expression. Here, we used a co-culture system using cell culture inserts, so that cell products can affect the other cell type without any contact signaling. The real-time PCR result showed that IL-1β mRNA level was high in B10 cells in respect to HMO6 (Fig. 6C), although at protein level the expression was similar among the cell types (Supplemental Fig. 3). In co-culture system, IL-1β mRNA was increased in B10 cells, whereas it was decreased in HMO6 after 36 h (Fig. 7C). However, VEGF mRNA level was increased in co-culture system in both cell types (Fig. 7D).

Next, we investigated about the effect of B10 cells on HIF-1α and VEGF proteins expression in HMO6 during oxygen-glucose deprivation (OGD) and non-OGD culture conditions. Western blotting results showed that compared to HMO6 native culture, VEGF protein level was increased in HMO6 co-cultured with B10 cells for 24 h, whereas HIF-1α protein level was not affected (Fig. 6E and F, non-OGD). OGD alone increased both HIF-1α and VEGF in HMO6 compared to native culture (Fig. 7E and F). However, co-culture with B10 did not affect such OGD-

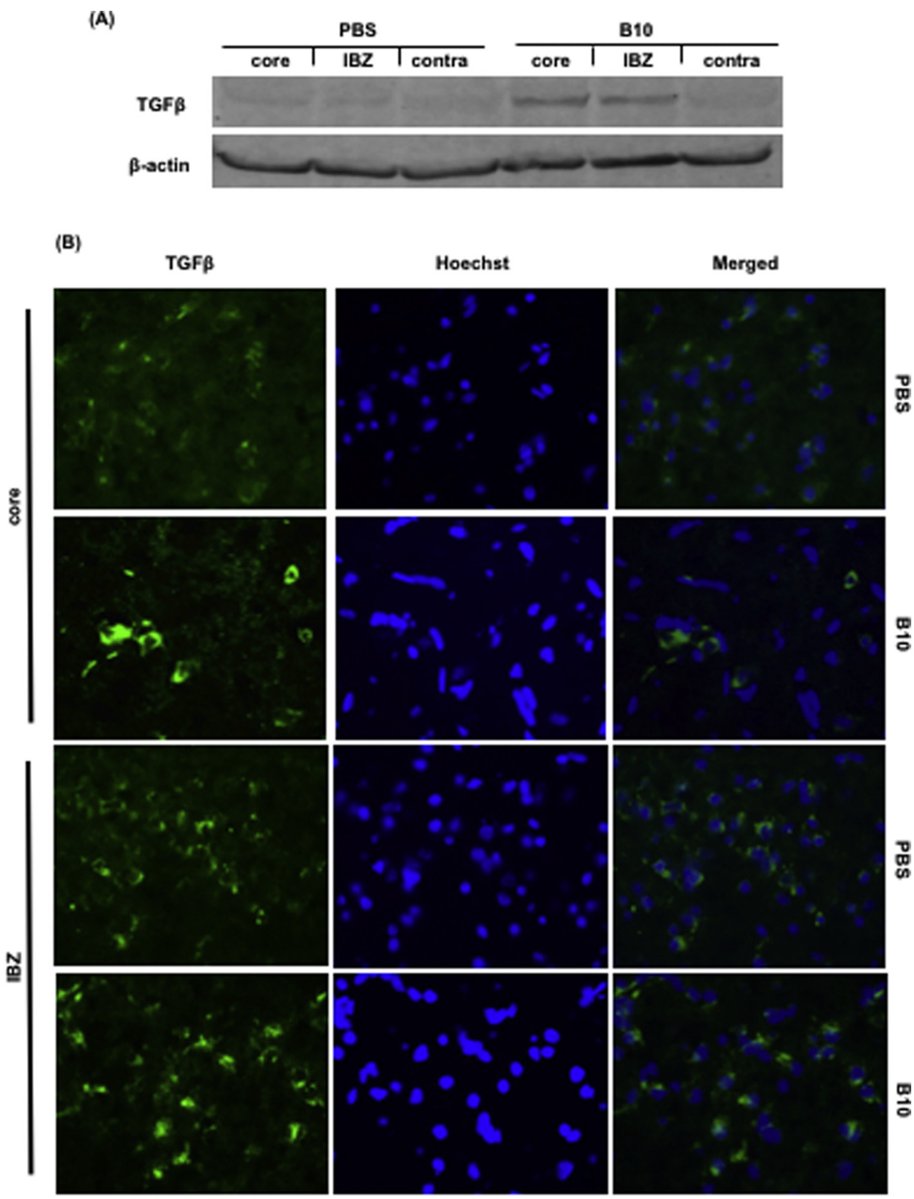

Fig. 6. Effects of B10 transplantation on TGFβ protein levels in MCAO rat brains. B10 cells were transplanted intravenously 24 h after MCAO. Control MCAO rats received PBS instead of cells. Three days after MCAO, cortical brain tissues from ischemic core, IBZ and contralateral areas were dissected out, and level of TGFβ was evaluated by Western blot analysis using specific antibody (A). β-Actin was used as a loading control (A). The protein expression was further evaluated by immunofluorescence staining using TGFβ-specific antibody. Representative photomicrographs of core, IBZ and contralateral cortical areas of PBS-treated and B10-transplanted MCAO rats are shown in (B). Hoechst was used for nuclear staining.

induced increment of HIF-1α and VEGF in HMO6 (Fig. 7E and F).

3.8. B10 transplantation regulated IL-1β production in a rat MCAO model

Next, we checked IL-1β expression in vivo in rat MCAO models. Our immunostaining results showed that IL-1β producing cells were found mainly in the core region of rats 3 days after MCAO, with some cells having low level of IL-1β in the IBZ (Fig. 8A and B). Counting immunoreactive cells revealed that the number of IL-1β positive cells was increased in B10-transplanted group (Fig. 8C). To identify the cells that produced IL-1β, we employed double immunofluorescence staining. The staining results showed that in PBS-treated rat MCAO model, IL-1β is expressed mainly in ED-1 positive macrophage/microglia (Fig. 8D). In B10-translanted group, IL-1β was expressed in ED-1 positive macrophage/microglia as well as in human nuclear antigen positive transplanted B10 cells (Fig. 8D and E).

3.9. Silencing IL-1β in B10 decreased its ability to induce endoglin in a rat MCAO model

To explore further about the role of IL-1β in B10-induced angiogenesis, we silenced its expression in B10 cells by mRNA specific siRNA transfection. IL-1β mRNA specific siRNA decreased the expression both at mRNA and protein level to < 40% (Supplemental Fig. 4). These IL-1β-silenced B10 cells were transplanted in rat MCAO model. Immunostaining results showed that endoglin positive area was significantly decreased in the core and IBZ regions of IL-1β-silenced B10 transplanted rats compared to non-silenced B10 transplanted rats both at 3 days (Fig. 9A and B) and 7 days (Fig. 9C and D) after MCAO. However, endoglin positive vessel-like structure appeared early in IL-β-silenced B10 transplanted rat brains, as early as 3 days after MCAO, which was not observed in non-silenced B10 transplanted condition (Fig. 9A and C).

4. Discussion

Vascular remodeling and angiogenesis plays a key role in the

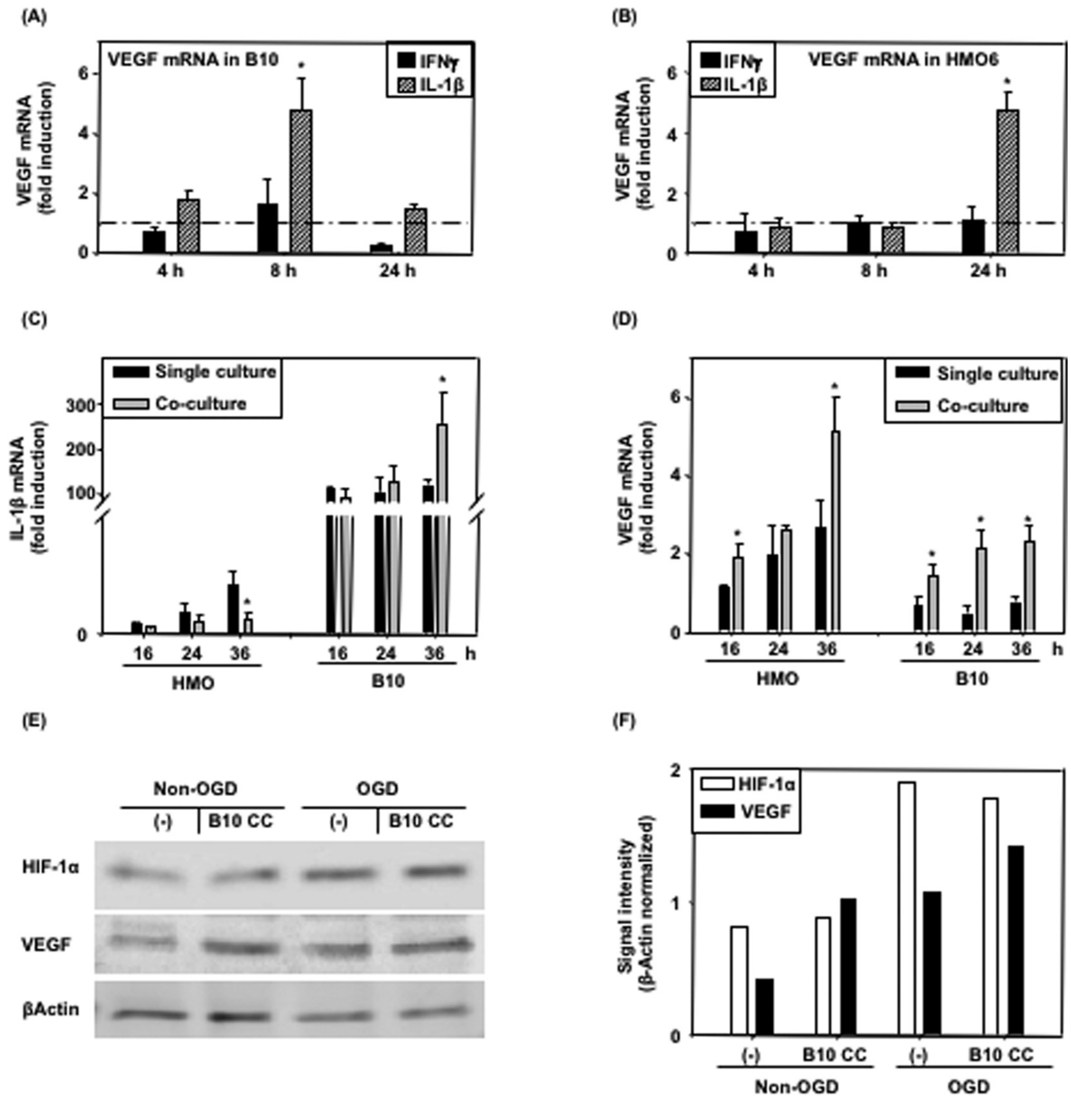

Fig. 7. Influence of B10 and microglia on the regulation of VEGF expression. B10 and HMO6 cells were treated with inflammatory cytokines for indicated times. After isolation of total RNA, cDNA was prepared, and VEGF mRNA levels in B10 (A) and HMO6 (B) were evaluated by real time PCR using gene specific primers. The mRNA was quantified as fold induction relative to medium-treated condition of same time points after normalization with corresponding GAPDH mRNA, and the results are presented as mean ± SEM of at least 3 independent experiments. Statistical significance is denoted as follows; $*p < 0.05$, vs medium-treated condition of same time point. (C and D) B10 and HMO6 were co-cultured in 0.5% FBS containing DMEM medium for indicated times. After isolation of total RNA, cDNA was prepared, and the mRNA levels of IL-1β (C) and VEGF (D) in B10 and HMO6 was determined by real time PCR. After normalization with corresponding GAPDH mRNA, the mRNA was quantified relatively using 1 sample of HMO6 normal culture as a calibrator. The data presented here as an average ± SD of 3 independent experiments. Statistical significance is denoted as follows; $*p < 0.05$, vs native culture condition of same time point. (E and F) HMO6 was treated 0.5% FBS containing DMEM for 24 h in native culture, or B10 co-culture (B10 CC) condition. Then the cell lysate was collected before, or 4 h of OGD. The levels of HIF1α and VEGF in HMO6 cell lysates were evaluated by Western blotting using specific antibodies. β-Actin was used as a loading control. A representative Western blotting data is shown in (E), and its β-Actin-normalized densitometric analysis is shown in (F).

pathological outcome of stroke condition (Krupinski et al. 1994; Lapi and Colantuoni 2015; Zhang and Chopp 2015). Experimental evidences suggested that a better vascular remodeling system improved not only the blood supply, but also neuronal function (Lapi and Colantuoni 2015). This fact is supported by the clinical observations that the stroke patients having better local circulation attain better outcome (Krupinski et al. 1994). In our previous study, we have demonstrated that B10 transplantation improves neurological performances of a rat MCAO model (Wakabayashi et al. 2010). In that study, we have found that the mRNA expression of VEGF-A was increased in MCAO rat brains at an earlier time point than other growth factors and cytokines. Importantly, compared to control, B10 transplantation increased VEGF-A mRNA in MCAO rat brains at that time point. Consistent with that finding, in this study we have demonstrated that B10 transplantation increased vessel density in the core and IBZ region from 3 days after MCAO. Besides, endoglin staining was increased in B10 transplantation condition, and the difference with PBS-treated MCAO rats was persisted after the disappearance of transplanted cells, signifying a lasting effect of transplantation on angiogenesis. Hence, early regulation of angiogenesis could be an important feature of B10 transplantation-mediated neurological improvement in MCAO condition.

VEGF family proteins including VEGF-A and PlGF are considered to be potent angiogenic factors (Holmes and Zachary 2005). Here, we have demonstrated VEGF-A at protein level and PIGF mRNA were increased by B10 transplantation, suggesting a central role of VEGF family proteins in MSC-mediated angiogenesis in cerebral ischemic condition. However, VEGF not only increases angiogenesis, but also reported to increase the vascular permeability leading to cerebral

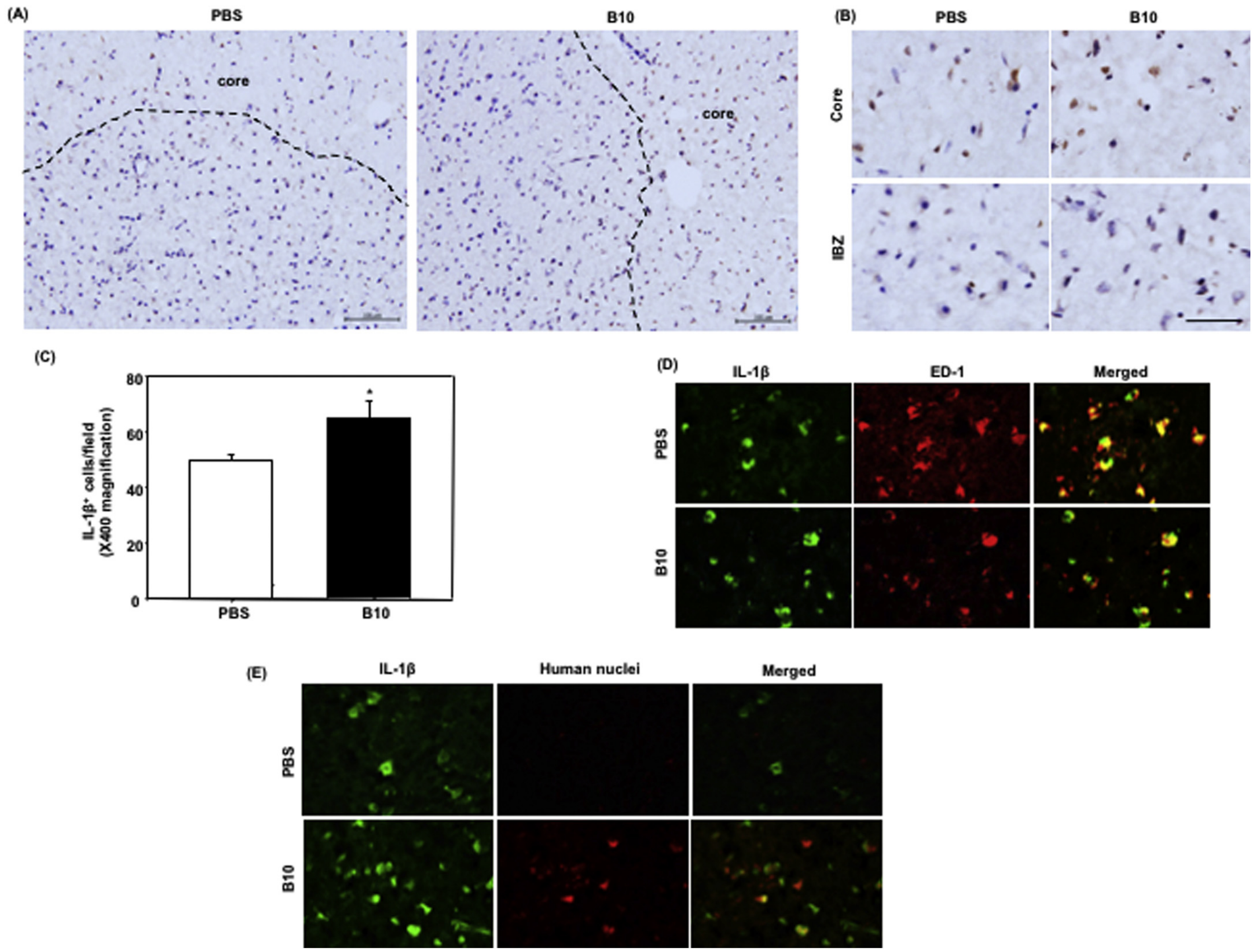

Fig. 8. Effects of B10 transplantation on IL-1β expression in MCAO rat brains. B10 cells were transplanted intravenously 24 h after MCAO. Control MCAO rats received PBS instead of cells. Three days after MCAO, the distribution of IL-1β-expressing cells are determined by immunostaining. Representative photomicrographs of PBS and B10 transplanted rats at low magnification are show in (A), where cortical core region is demarcated by dashed lines. Higher magnification of photomicrographs of core and IBZ region are shown in (B). Immunoreactive cells are counted in the core region at X400 magnification, and the data are presented as average ± SD of 5 rats in (C). To determine IL-1β expressing cells in the core, double immunofluorescence staining was done where ED-1 and human nuclear antigen were used as macrophage/microglia and transplanted B10 cell marker, respectively. Representative photomicrographs of double immunofluorescence staining of IL-1β and ED-1 in PBS and B10 transplanted rats are shown in (D). Double immunofluorescence staining of IL-1β and human nuclear antigen in PBS and B10 transplanted rats are shown in (E). Statistical significance is denoted as follows; $*p < 0.05$, vs PBS (control) rats. Bar = 100 μm in (A), and 50 μm in (B).

edema (Zhang et al. 2000). Our real-time PCR results showed that along with VEGF, B10 transplantation increased angiopoetin1 (Ang1) expression in IBZ region. Ang1 is considered to stabilize newly formed vessels through the activation of Tie2 receptor during angiogenesis (Brindle et al. 2006; Fiedler and Augustin 2006). Ang1-mediated Tie2 activation is reported to be antagonized by Ang2 (Maisonpierre et al. 1997; Scharpfenecker 2005). Interestingly the mRNA level of Ang2 was high in PBS group compared to B10 transplanted MCAO rats in IBZ area. This finding indicates that Ang1-Tie2 dependent new vessel stabilization could be well achieved in B10 transplanted condition. Moreover, TGFβ expression was increased in B10 transplanted MCAO rats. TGFβ is demonstrated to regulate angiogenesis in concert with VEGF, and it is also shown that abrogation of the interaction of VEGF and TGFβ caused abnormal vessel formation (Ferrari et al. 2009). Hence, B10 transplantation might regulate the process of angiogenesis along with stabilization of newly formed vessels, and provides better perfusion efficiency.

In ischemic condition, VEGF expression is mainly regulated by HIF-1α, a hypoxia regulated transcription factor (Chen et al. 2010). In our study, we found that HIF-1α mRNA as well as protein was increased in B10 transplanted rat brains. In normoxia, HIF-1α becomes a target of proteasome system by prolyl hydroxylases and rapidly degraded (Salceda and Caro 1997). In hypoxic condition, the activity of prolyl hydroxylase is inhibited, casing stabilization of HIF-1α (Jaakkola et al. 2001). Although we did not investigate about the enzyme activity, the mRNA expression of prolyl hydroxylases EGLN1, EGLN2 and EGLN3 was not changed in B10 transplanted rats. In OGD condition, HIF-1α protein level is known to increase due to decreased activity of prolyl hydroxylases (Souvenir et al. 2014). In our culture condition, HIF-1α protein level in native cultured and B10 co-cultured HMO6 were similarly increased after OGD, indicating that B10 did not affect prolyl hydroxylase enzyme activity in HMO6. Therefore, B10 transplantation might not increase HIF-1α protein through inhibiting EGLNs, rather by regulating its transcription.

In B10 transplanted rats, we have found that both HIF-1α and VEGF were expressed in the core and IBZ regions. VEGF is reported to be express in astrocytes, neurons and microglia (Greenberg and Jin 2013). However, soon after stroke, microglia are considered to be the main

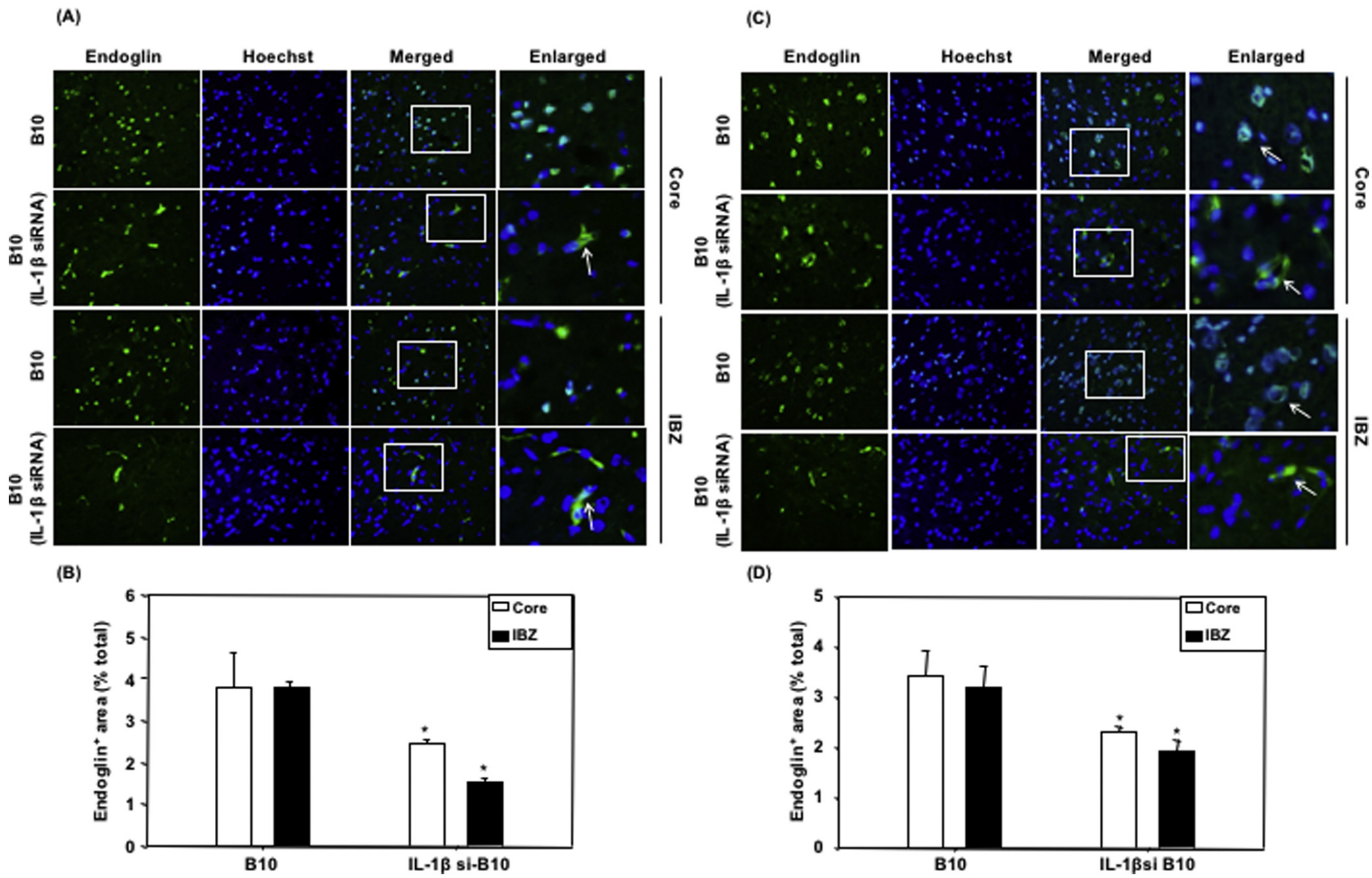

Fig. 9. Effects of IL-1β-silenced B10 transplantation on the newly formed vessels in MCAO rat brains. IL-1β-silenced B10, or non-silenced B10 cells were transplanted intravenously 24 h after MCAO. Three and 7 days after MCAO, newly formed vessels in the core and IBZ region were visualized by endoglin immunofluorescence staining. The density of newly formed vessels was evaluated using ImageJ, as described in the Materials and Methods, and expressed as percent of total area of a microscopic field at x400 magnification. Representative endoglin immunofluorescence staining photomicrographs of ischemic core and IBZ cortices of rat brains 3 and 7 days after MCAO are shown in (A) and (C), respectively. Boxed area of the merged photomicrographs are enlarged and shown in 4th column. Vessel-like structures are indicated by arrows. Quantified data of the staining of rat brains 3 (B) and 7 (D) days after MCAO are presented as average of 5 rats ± SD. Statistical significance are denoted as follows; *$p < 0.01$ vs same area of non-silenced B10 transplanted MCAO rats.

source of VEGF (Greenberg and Jin 2013). In this study, we demonstrated that although HIF-1α expressed both in astrocytes and macrophage/microglia, VEGF was rarely found to be positive in astrocytes during this early time point, indicating the time-dependent role of different cell-types in angiogenesis (Greenberg and Jin 2013). In a previous study, we have found that B10 transplantation decreased total number of macrophage/microglia in the core and IBZ regions of MCAO rats (Sheikh et al. 2011), suggesting a possibility that total VEGF expression might be decreased by B10 transplantation. However, microglia of M2 phenotype are demonstrated to express VEGF (Lamagna et al. 2006). In our previous studies (Sheikh et al. 2011; Wakabayashi et al. 2010), we showed that B10 transplantation not only increased VEGF, IL-10 and IL-4, but also decreased iNOS. These facts might imply that although it decreases the total macrophage/microglia cell number, it influences their M2 transition, and thereby increases VEGF and angiogenic factors expression. Such M2 transition of macrophage/microglia could be important for early angiogenesis and reparative processes, and subsequent neurological improvement that are seen in B10-transplanted condition.

As inflammation and angiogenesis are intimately related (Asano-Kato et al. 2005; Parmeggiani et al. 2010), we focused to investigate whether MSC transplantation modulates angiogenesis process through the regulation of inflammatory cytokines. Our real-time PCR and ELISA results showed that IL-1β expression was high in B10 cells. Also, IL-1β time-dependently increased VEGF mRNA expression in both B10 and a human microglia cell line (HMO6). Interestingly, co-culture of B10 and HMO6 increased IL-1β in B10, but decreased it in HMO6 cells. In a previous study, we showed that B10 transplantation increased IL-1β mRNA slightly in the core region at 3 days, and significantly in the IBZ region at 7 days after MCAO. In this study, IL-1β expressing cells were found to be modestly, but significantly increased in B10 transplanted rats 3 days after MCAO, where many of the IL-1β expressing cells were transplanted B10. These results are suggesting that B10 could be an important source of IL-1β in B10 transplanted MCAO rats, which increases endothelial cell proliferation and angiogenesis in the animal model (Yang et al. 2012; Voronov et al. 2003). The results of silencing study proved that hypothesis, since inhibiting expression of IL-1β in B10 cells decreases endoglin positive area in MCAO rat brains. Interestingly, vessel-like structure appeared early in IL-1β-silenced B10 transplanted rat brains, suggesting that although it increases endothelial cell proliferation, IL-1β might have a negative effect on vessel-like structure formation. In addition to its effects on proliferation, previous studies have demonstrated a role of IL-1β on endothelial cell apoptosis (Rivera et al. 2013; Zhu et al. 2014). Hence, a controlled expression of IL-1β could be important for proper angiogenesis, where an endothelial proliferation, apoptosis, arrangement to vessel-like structure and maturation are balanced. It will be interesting to investigate further about the role of IL-1β, and its interaction with the factors expressed by B10 cells that mediated angiogenesis in vivo in cerebral ischemic condition.

In conclusion, our findings provide a new insight of the mechanism of angiogenesis in cerebral ischemia condition, its regulation by mesenchymal stem cell transplantation and the importance of IL-1β on that regulation. Such understanding could be valuable for the improvement of stroke therapy.

Conflict of interest

References

Asano-Kato, N., Fukagawa, K., Okada, N., Kawakita, T., Takano, Y., Dogru, M., Tsubota, K., Fujishima, H., 2005. TGF-beta1, IL-1beta, and Th2 cytokines stimulate vascular endothelial growth factor production from conjunctival fibroblasts. Exp. Eye Res. 80, 555–560.

Bakopoulou, A., Kritis, A., Andreadis, D., Papachristou, E., Leyhausen, G., Koidis, P., Geurtsen, W., Tsiftsoglou, A., 2015. Angiogenic potential and secretome of human apical papilla mesenchymal stem cells in various stress microenvironments. Stem Cells Dev. 24, 2496–2512.

Bang, O.Y., Goyal, M., Liebeskind, D.S., Najm, M., Rubiera, M., Fainardi, E., 2015. Collateral circulation in ischemic stroke: assessment tools and therapeutic strategies. Stroke 46, 3302–3309.

Bélanger, M., Allaman, I., Magistretti, P.J., 2011. Brain energy metabolism: focus on Astrocyte-neuron metabolic cooperation. In: Cell Metabolism. vol. 14. pp. 724–738.

Brindle, N.P.J., Saharinen, P., Alitalo, K., 2006. Signaling and functions of angiopoietin-1 in vascular protection. In: Circulation Research. vol. 98. pp. 1014–1023.

Buga, A.M., Margaritescu, C., Scholz, C.J., Radu, E., Zelenak, C., Popa-Wagner, A., 2014. Transcriptomics of post-stroke angiogenesis in the aged brain. Front. Aging Neurosci. 6.

Carmeliet, P., Jain, R.K., 2011. Molecular mechanisms and clinical applications of angiogenesis. Nature 473, 298–307.

Ceulemans, A.G., Zgavc, T., Kooijman, R., Hachimi-Idrissi, S., Sarre, S., Michotte, Y., 2010. The dual role of the neuroinflammatory response after ischemic stroke: modulatory effects of hypothermia. J. Neuroinflammation 7, 74.

Chen, J., Li, Y., Katakowski, M., Chen, X., Wang, L., Lu, D., Lu, M., Gautam, S.C., Chopp, M., 2003. Intravenous bone marrow stromal cell therapy reduces apoptosis and promotes endogenous cell proliferation after stroke in female rat. J. Neurosci. Res. 73, 778–786.

Chen, J., Li, Y., Zhang, R., Katakowski, M., Gautam, S.C., Xu, Y., Lu, M., Zhang, Z., Chopp, M., 2004. Combination therapy of stroke in rats with a nitric oxide donor and human bone marrow stromal cells enhances angiogenesis and neurogenesis. Brain Res. 1005, 21–28.

Chen, C., Ostrowski, R.P., Zhou, C., Tang, J., Zhang, J.H., 2010. Suppression of hypoxia-inducible factor-1α and its downstream genes reduces acute hyperglycemia-enhanced hemorrhagic transformation in a rat model of cerebral ischemia. J. Neurosci. Res. 88, 2046–2055.

Ferrari, G., Cook, B.D., Terushkin, V., Pintucci, G., Mignatti, P., 2009. Transforming growth factor-beta 1 (TGF-beta1) induces angiogenesis through vascular endothelial growth factor (VEGF)-mediated apoptosis. J. Cell. Physiol. 219, 449–458.

Fiedler, U., Augustin, H.G., 2006. Angiopoietins: a link between angiogenesis and inflammation. In: Trends in Immunology. Vol. 27. pp. 552–558.

Forsythe, J.A., Jiang, B.H., Iyer, N.V., Agani, F., Leung, S.W., Koos, R.D., Semenza, G.L., 1996. Activation of vascular endothelial growth factor gene transcription by hypoxia-inducible factor 1. Mol. Cell. Biol. 16, 4604–4613.

Greenberg, D.A., Jin, K., 2013. Vascular endothelial growth factors (VEGFs) and stroke. Cell. Mol. Life Sci. 70, 1753–1761.

Holmes, D.I.R., Zachary, I., 2005. The vascular endothelial growth factor (VEGF) family: angiogenic factors in health and disease. Genome Biol. 6, 209.

Jaakkola, P., Mole, D.R., Tian, Y.M., Wilson, M.I., Gielbert, J., Gaskell, S.J., von Kriegsheim, A., Hebestreit, H.F., Mukherji, M., Schofield, C.J., Maxwell, P.H., Pugh, C.W., Ratcliffe, P.J., 2001. Targeting of HIF-alpha to the von Hippel-Lindau ubiquitylation complex by O2-regulated prolyl hydroxylation. Science 292, 468–472.

Krupinski, J., Kaluza, J., Kumar, P., Kumar, S., Wang, J., 1994. Role of angiogenesis in patients with cerebral ischemic stroke. Stroke 25, 1794–1798.

Kumar, V., Abbas, A.K., Fausto, N., Aster, J.C., 2010. Robbins and Cotran Pathologic Basis of Disease. pp. 23–24.

Lamagna, C., Aurrand-Lions, M., Imhof, B.a., 2006. Dual role of macrophages in tumor growth and angiogenesis. J. Leukoc. Biol. 80, 705–713.

Lapi, D., Colantuoni, A., 2015. Remodeling of Cerebral Microcirculation after Ischemia-Reperfusion. J. Vasc. Res. 52, 22–31.

Liebeskind, D.S., 2003. Collateral circulation. In: Stroke. vol. 34. pp. 2279–2284.

Maisonpierre, P.C., Suri, C., Jones, P.F., Bartunkova, S., Wiegand, S.J., Radziejewski, C., Compton, D., McClain, J., Aldrich, T.H., Papadopoulos, N., Daly, T.J., Davis, S., Sato, T.N., Yancopoulos, G.D., 1997. Angiopoietin-2, a natural antagonist for Tie2 that disrupts in vivo angiogenesis. Science 277, 55–60.

Nagai, a, Nakagawa, E., Hatori, K., Choi, H.B., McLarnon, J.G., Lee, M.a., Kim, S.U., 2001. Generation and characterization of immortalized human microglial cell lines: expression of cytokines and chemokines. Neurobiol. Dis. 8, 1057–1068.

Nagai, A., Kim, W.K., Lee, H.J., Jeong, H.S., Kim, K.S., Hong, S.H., Park, I.H., Kim, S.U., 2007. Multilineage potential of stable human mesenchymal stem cell line derived from fetal marrow. PLoS One 2.

Nguyen, H.-L., Lee, Y.J., Shin, J., Lee, E., Park, S.O., McCarty, J.H., Oh, S.P., 2011. TGF-β signaling in endothelial cells, but not neuroepithelial cells, is essential for cerebral vascular development. Lab. Investig. 91, 1554–1563.

Ohab, J.J., Fleming, S., Blesch, A., Carmichael, S.T., 2006. A neurovascular niche for neurogenesis after stroke. J. Neurosci. 26, 13007–13016.

Parmeggiani, F., Campa, C., Costagliola, C., Incorvaia, C., Sheridan, C., Semeraro, F., De Nadai, K., Sebastiani, A., 2010. Inflammatory mediators and angiogenic factors in choroidal neovascularization: pathogenetic interactions and therapeutic implications. Mediat. Inflamm. 2010.

Rivera, J.C., Sitaras, N., Noueihed, B., Hamel, D., Madaan, A., Zhou, T., Honoré, J.C., Quiniou, C., Joyal, J.S., Hardy, P., Sennlaub, F., Lubell, W., Chemtob, S., 2013. Microglia and interleukin-1β in ischemic retinopathy elicit microvascular degeneration through neuronal semaphorin-3A. Arterioscler. Thromb. Vasc. Biol. 33, 1881–1891.

Ruas, J.L., Berchner-Pfannschmidt, U., Malik, S., Gradin, K., Fandrey, J., Roeder, R.G., Pereira, T., Poellinger, L., 2010. Complex regulation of the transactivation function of hypoxia-inducible factor-1αby direct interaction with two distinct domains of the creb-binding protein/p300. J. Biol. Chem. 285, 2601–2609.

Salceda, S., Caro, J., 1997. Hypoxia-inducible factor 1α (HIF-1α) protein is rapidly degraded by the ubiquitin-proteasome system under normoxic conditions. Its stabilization by hypoxia depends on redox-induced changes. J. Biol. Chem. 272, 22642–22647.

Scharpfenecker, M., 2005. The Tie-2 ligand Angiopoietin-2 destabilizes quiescent endothelium through an internal autocrine loop mechanism. J. Cell Sci. 118, 771–780.

Sheikh, A.M., Nagai, A., Wakabayashi, K., Narantuya, D., Kobayashi, S., Yamaguchi, S., Kim, S.U., 2011. Mesenchymal stem cell transplantation modulates neuroinflammation in focal cerebral ischemia: contribution of fractalkine and IL-5. Neurobiol. Dis. 41, 717–724.

Souvenir, R., Flores, J.J., Ostrowski, R.P., Manaenko, A., Duris, K., Tang, J., 2014. Erythropoietin inhibits HIF-1?? expression via upregulation of PHD-2 transcription and translation in an in Vitro model of hypoxia-ischemia. Transl Stroke Res 5, 118–127.

Sun, Y., Jin, K., Xie, L., Childs, J., Mao, X.O., Logvinova, A., Greenberg, D.A., 2003. VEGF-induced neuroprotection, neurogenesis, and angiogenesis after focal cerebral ischemia. J. Clin. Investig. 111, 1843–1851.

Thored, P., Wood, J., Arvidsson, A., Cammenga, J., Kokaia, Z., Lindvall, O., 2007. Long-term neuroblast migration along blood vessels in an area with transient angiogenesis and increased vascularization after stroke. Stroke 38, 3032–3039.

Voronov, E., Shouval, D.S., Krelin, Y., Cagnano, E., Benharroch, D., Iwakura, Y., Dinarello, C.A., Apte, R.N., 2003. IL-1 is required for tumor invasiveness and angiogenesis. Proc. Natl. Acad. Sci. U. S. A. 100, 2645–2650.

Wakabayashi, K., Nagai, A., Sheikh, A.M., Shiota, Y., Narantuya, D., Watanabe, T., Masuda, J., Kobayashi, S., Kim, S.U., Yamaguchi, S., 2010. Transplantation of human mesenchymal stem cells promotes functional improvement and increased expression of neurotrophic factors in a rat focal cerebral ischemia model. J. Neurosci. Res. 88, 1017–1025.

Wang, M.M., Klaus, J.a., Joh, H.-D., Traystman, R.J., Hurn, P.D., 2002. Postischemic angiogenic factor expression in stroke-prone rats. Exp. Neurol. 173, 283–288.

Wang, H., Nagai, A., Sheikh, A.M., Liang, X.Y., Yano, S., Mitaki, S., Ishibashi, Y., Kobayashi, S., Kim, S.U., Yamaguchi, S., 2013. Human mesenchymal stem cell transplantation changes proinflammatory gene expression through a nuclear factor-κB-dependent pathway in a rat focal cerebral ischemic model. J. Neurosci. Res. 91, 1440–1449.

Xiong, Y., Mahmood, A., Chopp, M., 2011. Angiogenesis, neurogenesis and brain recovery of function following injury. Curr. Opin. Investig. Drugs 11, 298–308.

Yang, L., Guo, X.G., Du, C.Q., Yang, J.X., Jiang, D.M., Li, B., Zhou, W.J., Zhang, F.R., 2012. Interleukin-1 beta increases activity of human endothelial progenitor cells: involvement of PI3K-Akt signaling pathway. Inflammation 35, 1242–1250.

Yao, Y., Kubota, T., Takeuchi, H., Sato, K., 2005. Prognostic significance of microvessel density determined by an anti-CD105/endoglin monoclonal antibody in astrocytic tumors: comparison with an anti-CD31 monoclonal antibody. Neuropathology 25, 201–206.

Zhang, Z.G., Chopp, M., 2015. Promoting brain remodeling to aid in stroke recovery. Trends Mol. Med. 21, 543–548.

Zhang, Z.G., Zhang, L., Jiang, Q., Zhang, R., Davies, K., Powers, C., Van Bruggen, N., Chopp, M., 2000. VEGF enhances angiogenesis and promotes blood-brain barrier leakage in the ischemic brain. J. Clin. Investig. 106, 829–838.

Zhu, X., Xie, M., Wang, K., Zhang, K., Gao, Y., Zhu, L., Zhou, F., 2014. The effect of puerarin against IL-1β-mediated leukostasis and apoptosis in retinal capillary endothelial cells (TR-iBRB2). Mol. Vis. 20, 1815–1823.